WELDING RESEARCH

SUPPLEMENT TO THE *WELDING JOURNAL*, AUGUST 1995
Sponsored by the American Welding Society and the Welding Research Council

RESEARCH/DEVELOPMENT/RESEARCH/DEVELOPMENT/RESEARCH/DEVELOPMENT/RESEARCH/DEVELOPMENT

Microstructure and Properties of Ferritic Steel Welds Containing Al and Ti

Titanium proves a strong influence on the formation of acicular ferrite

BY G. M. EVANS

ABSTRACT. The combined effect of Al and Ti, in the range 5 to 500 ppm, on the microstructure and properties of C-Mn shielded metal arc welds has been studied. It was found that Ti, in contrast to Al, dramatically enhanced the formation of acicular ferrite and improved notch toughness. A strong interactive effect was encountered, with Al at low concentrations tending to diminish the influence of Ti. Unless a critical balance is achieved, with regard to oxygen content, it is concluded that Ti be optimized at 30 to 40 ppm and that Al be kept as low as possible.

Introduction

This study forms part of an ongoing program to evaluate the influence of microalloying elements in ferritic shielded metal arc deposits. Previous work (Ref. 1) has evaluated the individual effects of Al, Ti, B, V and Nb on the toughness of high-purity weld metal, and it is now expedient to investigate interactive phenomena, starting with the Al-Ti system.

Elements in isolation were found (Ref. 1) to exhibit a complex effect on weld metal toughness, with titanium being the most potent. An exploratory study (Ref. 2) had previously revealed that the transfer of a small amount of Ti into the deposit, of the order of 30 ppm, dramatically modified the weld metal microstructure and properties. The effect of titanium, however, was subsequently (Ref. 3) established to be influenced by the amount of manganese required to generate the correct degree of hardenability. The balance was such that optimum properties were achieved at 1.4% Mn, in combination with 30 to 40 ppm Ti. Following degradation, at intermediate Ti levels, impact toughness again improved to yield another optimum at titanium contents in excess of 200 ppm. A parallel study (Ref. 4) at that time of the effects of aluminum in combination with 36 to 44 ppm Ti showed that Al modified microphase morphology and changed the average composition of the nonmetallic inclusions without noticeably altering their mean diameter. The present intention was to include and repeat the latter test series at different nominal Ti levels so as to assess the combined matrix of both elements in the range from 5 up to approximately 500 ppm.

The relevant literature deals otherwise only sparingly with the role of titanium and aluminum in shielded metal arc deposits (Refs. 5, 6), whereas, extensive studies have been conducted on submerged arc (Refs. 7–19) and gas metal arc (GMA) weldments (Refs. 20–25) from solid wires. An evident lack of information also existed for tubular cored wire deposits until Abson (Ref. 26) added controlled amounts of aluminum to metal cored and flux cored welding wires. High aluminum contents were deleterious, and it was concluded that the development of as-deposited microstructures was governed by considerations which were essentially the same as those found to apply to submerged arc welds (Ref. 27). A consequence of adding aluminum, however, was that a simultaneous drift in titanium was encountered, thus obscuring to a certain extent the individual trends. The present work attempts to balance the combined system, using covered electrodes, with the intention of generating information, which hopefully can also be applied to other processes that operate over approximately the same weld metal oxygen range.

Key Words

Al-Ti System
Microalloying Elem.
Consumables
Microstructure
Low-Carbon Steel
Weld Metal
Ferritic Steel Welds
Acicular Ferrite
SMAW
Notch Toughness

G. M. EVANS is with Oerlikon, Zurich, Switzerland. Paper presented at the AWS 74th Annual Meeting, April 25–29, 1993, Houston, Tex.

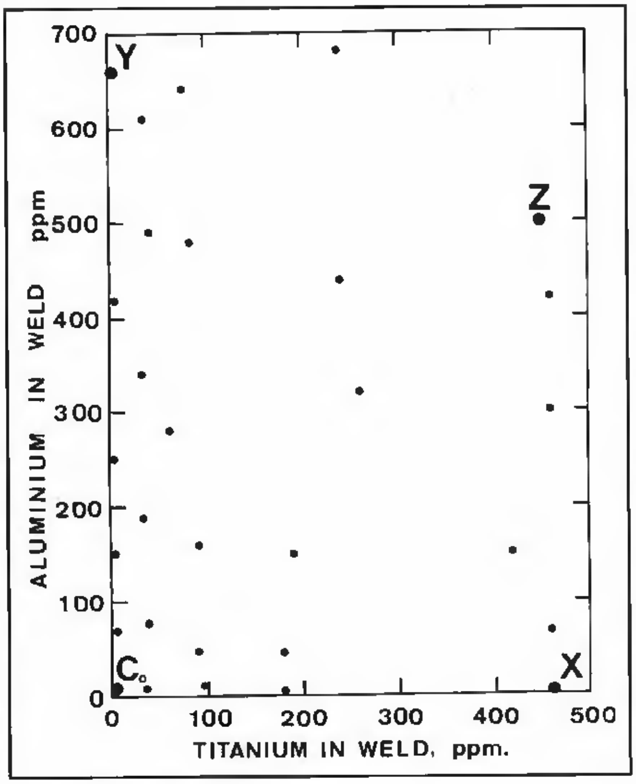

Fig. 1 — Plot of Al-Ti combinations.

Experimental Procedure

Electrodes

Increasing amounts of Al powder were added to the coatings of basic low-hydrogen electrodes to yield six nominal weld metal aluminum levels, namely 5, 60, 160, 300, 450 and 600 ppm Al, as described previously (Ref. 4).

Differing amounts of Ti metal powder were also added to produce five distinct sets of weldments containing the following nominal titanium contents, namely 5, 40, 80, 220 and 450 ppm Ti.

The electrodes were formulated in an attempt to maintain comparative levels of Al and Ti, and also keep C, Mn and Si constant. This necessitated, for a specific series, that the amount of graphite, manganese metal, ferrosilicon and Ti metal in the coating be progressively reduced as Al was added.

The core wire diameter of the 30 batches of experimental electrodes thus prepared was 4 mm (5/32 in.) and the coating factor (D/d) was 1.68.

Weld Preparation

The joint geometry was that specified in ISO 2560-1973. Welding was done in the flat position and three beads per layer were deposited, as described previously (Refs. 28, 37). The total number of runs required to fill the individual joints was 27. Direct current (electrode positive) was employed, the amperage being 170 A, the voltage 21 V and the heat-input was nominally 1 kJ/mm. The interpass temperature was standardized at 200°C (392°F).

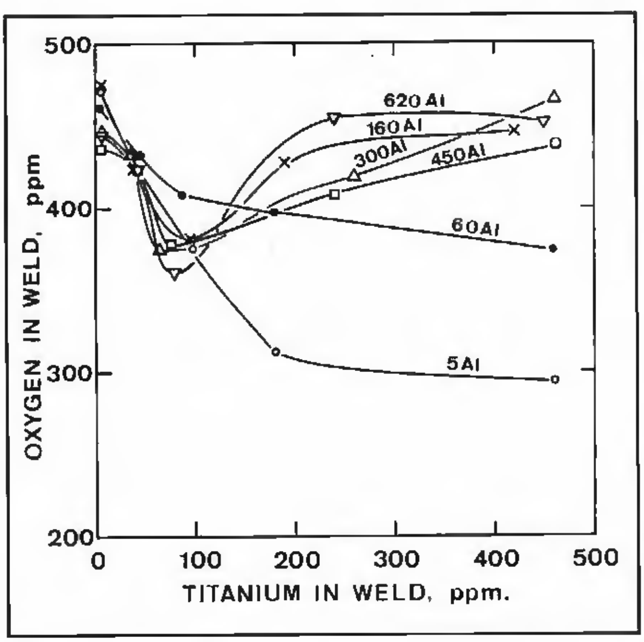

Fig. 2 — Plot of weld metal oxygen content vs. weld metal titanium content (different Al levels).

Mechanical Testing

Two subsize all-weld-metal tensile specimens (Minitrac) were machined and tested for each of the different deposits. Also, approximately 35 Charpy V-notch specimens were struck in each case, to obtain full transition curves. The tensile specimens were given a hydrogen removal treatment at 250°C (482°F) for 14 h, whereas, the Charpy specimens were tested in the as-welded condition (Ref. 28).

Metallography

Transverse sections of selected welds were prepared and detailed optical examination was carried out on the top beads and on the adjacent supercritically reheated zones, as in previous work (Ref. 28).

Results

Chemical Composition

The chemical analyses of the 30 all-weld-metal deposits are given in Table 1. The second series (40 ppm Ti) is derived from published work (Ref. 4), and on comparison, it is seen that the same unfortunate trend existed throughout, namely, for silicon to drift upward as aluminum increased. Carbon, manganese and titanium were relatively well balanced. As noted previously (Ref. 4), weld metal nitrogen decreased with increasing aluminum, a phenomenon attributed to a lowering of the nitrogen partial pressure by aluminum vapor in the arc atmosphere. The experimental combinations of aluminum and titanium studied are plotted in Fig. 1, with the extremes being designated as Co, X, Y and Z. Insufficient aluminum was added to the latter, the yield being 500 ppm Al rather than the intended 600 ppm. Titanium was generally invariable in the last series but less so in the preceding series (200 ppm Ti).

The oxygen content is plotted against weld metal titanium content in Fig. 2. A reversal is seen to have occurred, with aluminum obviating the oxidizing potential of the titanium. Of note, as reported previously (Ref. 4), is the fact that at 40 ppm Ti, the oxygen content remained insensitive to changes in aluminum level due to an evident balance.

Metallographic Examination

As-Deposited Weld Metal

The top beads of the deposits were optically examined and metallographic measurements were made, following the current guidelines (Ref. 29) of IIW Subcommission IX J, to quantify the major microstructural components, namely: primary ferrite (PF), ferrite with second phase (FS), and acicular ferrite (AF).

The point count results obtained for four of the test series are presented in Fig. 3. The microalloy-free deposit (Co) was essentially nonacicular, and it is seen that the introduction of aluminum in isolation

Table 1 — Weld Metal Analysis

Nominal Ti ppm	C	Mn	Si	S	P	N[a]	O[b]	Al[c]	Ti[c]
	%					ppm			
5	0.074	1.49	0.29	0.006	0.013	72	471	6	5
	0.081	1.43	0.29	0.006	0.013	54	461	60	5
	0.076	1.36	0.34	0.005	0.011	57	476	150	5
	0.079	1.37	0.39	0.005	0.011	47	446	250	5
	0.078	1.40	0.44	0.004	0.011	44	436	420	5
	0.081	1.42	0.48	0.004	0.006	46	444	660	4
40	0.069	1.36	0.30	0.007	0.009	68	432	5	37
	0.080	1.41	0.33	0.006	0.009	55	432	78	43
	0.076	1.36	0.37	0.005	0.009	53	422	190	36
	0.078	1.31	0.44	0.005	0.008	50	431	340	36
	0.076	1.30	0.51	0.005	0.008	48	423	490	43
	0.079	1.32	0.57	0.004	0.008	52	422	610	38
80	0.074	1.50	0.32	0.006	0.006	89	375	8	99
	0.074	1.41	0.27	0.007	0.006	70	407	47	88
	0.071	1.36	0.39	0.005	0.009	52	381	160	92
	0.069	1.36	0.45	0.005	0.008	44	374	280	63
	0.069	1.39	0.51	0.004	0.008	41	379	480	69
	0.072	1.40	0.57	0.004	0.008	38	360	640	80
220	0.081	1.54	0.34	0.007	0.008	80	312	3	180
	0.072	1.32	0.24	0.006	0.008	68	397	47	180
	0.072	1.33	0.34	0.006	0.008	57	427	150	190
	0.074	1.36	0.41	0.005	0.005	49	418	320	260
	0.066	1.41	0.46	0.004	0.009	49	407	440	240
	0.066	1.33	0.44	0.004	0.008	49	454	680	240
450	0.069	1.49	0.43	0.004	0.005	77	294	1	460
	0.071	1.44	0.36	0.007	0.005	94	373	67	460
	0.071	1.39	0.42	0.007	0.005	65	446	150	420
	0.071	1.44	0.52	0.005	0.005	67	466	300	460
	0.069	1.41	0.54	0.005	0.005	58	439	420	460
	0.067	1.40	0.57	0.005	0.005	60	451	500	450

Nb, V and B <5 ppm, 50 ppm Mo, Ni, Cr, Cu = 300 ppm.
a) LECO, b) BALZERS, c) ICP-AES.

caused a twofold increase in the volume fraction of AF, from 10 to 20%. In contrast, the addition of 40 ppm Ti induced a sevenfold increase in AF, and aluminum subsequently induced complex changes (Ref. 4), with an initial decrease in AF being followed by an increase and then by a substantial decrease again. At 200 ppm Ti, the initial reduction in AF persisted, at approximately 50 ppm Al, but at high Al contents little change in AF was encountered. Similarly, the highest Ti level studied (450 ppm Ti) showed only a marginal response to Al, with AF increasing slightly, at the expense of ferrite with second phase, at concentrations above 300 ppm Al.

Photomicrographs of as-deposited columnar regions of the four extreme compositional variants, Co, X, Y and Z, are shown in Fig. 4. The distinctive ability of titanium (X) to induce an acicular structure is clearly apparent, whereas Y, containing the maximum amount of Al, remained essentially bainitic. The mixed system (Z) is also observed to be acicular in character, with a high volume fraction of microphase. Further detail is revealed, at a higher magnification, in Fig. 5, with Z additionally showing the presence of large cubic particles.

Reheated Weld Metal

Optical examination of the high-temperature reheated regions directly below the top heads also revealed marked microstructural differences, as illustrated, for the extreme compositions in Fig. 6. At the high Ti level (X), the ferrite envelopes delineating the prior austenite grain boundaries were well defined and the structure was predominantly acicular. Aluminum addition in isolation (Y) resulted in relatively narrow ferrite envelopes, and the structure remained as ferrite with aligned M-A-C. In the mixed system, (Z), the ferrite envelopes were eliminated to a certain extent, and the grain interiors were principally transformed to ferrite with second phase.

The microstructure of the low-temperature reheated regions was also modified as a result of microalloying, with grain refinement and a change in microphase morphology being observed — Fig. 7. Titanium addition (X) led to less cementite film and the formation of degenerate pearlite (B/P) and M/A. Aluminum additions caused the so-called fine-grained regions to become more duplex in character, as observed previously (Ref. 4). The mixed system (Z) naturally retained the large cubic particles and on replication both single and multiple types were found, as shown in Fig. 8. Of note was also the presence, in cross-section, of small triangular-shaped protuberances. EDAX analysis of a number of particles revealed them to be complex Al/Ti compounds, probably oxides. Wide compositional differences existed, however, the variation being from Al rich through to Ti rich, as seen in Table 2.

Mechanical Properties

Tensile Results

The tensile test results are given in Table 3. The yield and the ultimate tensile strengths are plotted against titanium content in Figs. 9 and 10, respectively. A complex situation is seen to exist with a peak effect at 40 ppm Ti disturbing the general progressive increase in strength. At intermediate aluminum contents a reduction of the tensile parameters also occurred. In view of the discontinuous effect of titanium at 40 ppm, no attempt was made to apply regression analysis to the data.

Impact Results

Charpy V-notch transition curves,

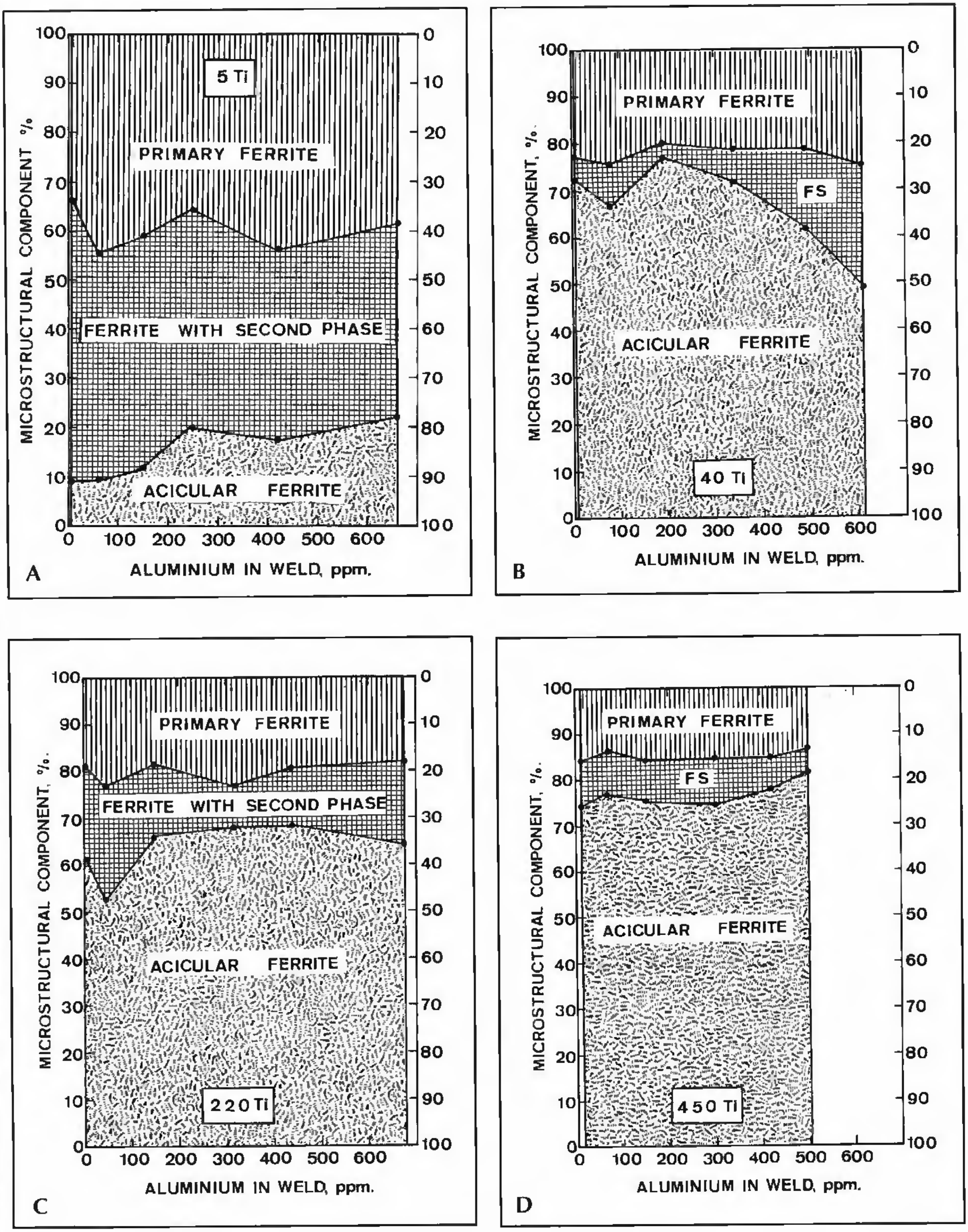

Fig. 3 — Effect of Al on the microstructure of as-deposited weld metal. A — 5 ppm Ti; B — 40 ppm Ti; C — 220 ppm Ti; D — 450 ppm Ti.

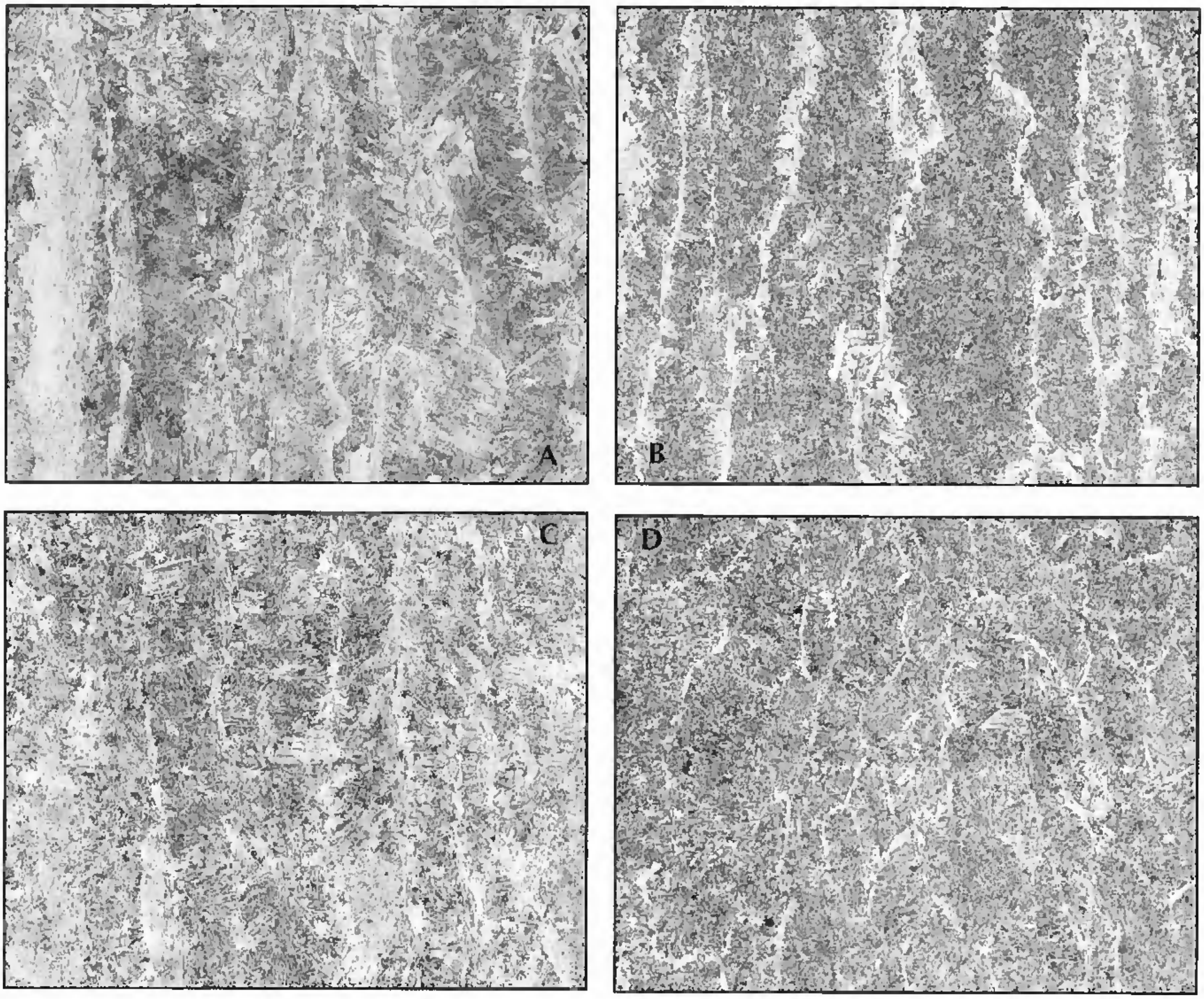

Fig. 4 — Photomicrographs of top beads (columnar). A — C_0 (6 Al, 5 Ti); B — X (1 Al, 460 Ti); C — Y (660 Al, 4 Ti); D — Z (500 Al, 450 Ti). 100X.

showing the effect of Ti at the six nominal aluminum levels, are plotted in Fig. 11. It is seen that the marked lateral shift of the curve to lower temperatures, incurred by the addition of titanium, was obviated by the addition of Al. Furthermore, a reduction in upper shelf energy produced a flattening of the Charpy transition curves.

The test temperatures corresponding to an absorbed energy of 100 J are plotted against aluminum content in Fig. 12A. A limited response is indicated for the titanium-free deposits, with a slight embrittling effect at 60 ppm Al. Considerable deterioration occurred at this concentration, for other titanium levels, and the subsequent improvement noted previously (Ref. 4) at 350 ppm Al was displaced toward 160 ppm Al as titanium increased. The same results are replotted in Fig. 12B, this time as a function of titanium, and reveal that the beneficial effect of a small amount of titanium was maintained up to a level of at least 450 ppm Al. The degradation encountered between 40 and 120 ppm Ti diminished with increasing aluminum and was eventually eliminated at 620 ppm Al.

An idealized three-dimensional model of the computerized data is presented in Fig. 13, with the steep vertical sidewall serving to illustrate the advantage gained by the addition of a trace amount of titanium. A further feature is the transverse ridge induced by aluminum, which culminates in a deleterious peak at 60 ppm Al and 100 ppm Ti. The combined system, at the experimental extreme, exhibits relatively poor toughness with little sensitivity to compositional change.

Discussion

The present work serves to confirm (Refs. 27, 30) the complex nature of ferritic weld metal, whereby, it is demonstrated that Al and Ti have different effects dependent on their relative presence. Hence, it is clear that dilution from the base plate could result in conflicting phenomena with different consumables and processes. By commencing with a microalloy-free deposit, in the present case, the opportunity was given of studying the elements both singly and in combination. In general, this is not possible since commercial consumables yield a certain amount of either one or both of the elements. For example, the behavior of a submerged arc flux would naturally depend on whether it was aluminate based or not. Similarly, a shielded metal arc electrode would respond differently to further addition when extruded onto an aluminum free "rimmed steel" wire than onto an aluminum killed wire produced by the concast route. Advances in analytical techniques and the realization of trace effects, especially at two distinct concentrations, requires a redefinition of the term "a small amount," as sometimes used in the past (Refs. 9, 11) to describe a level of 0.04 wt-

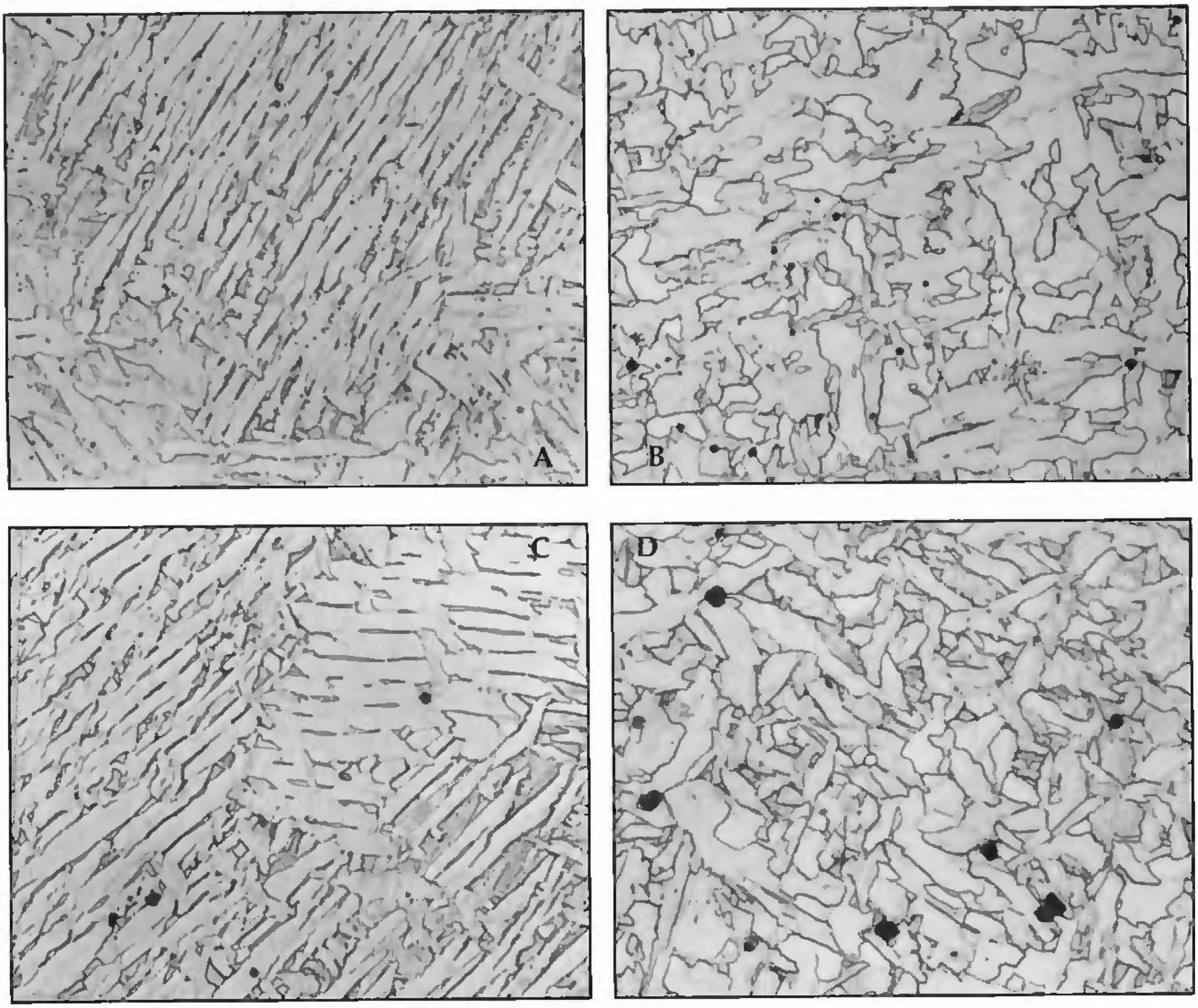

Fig. 5 — Photomicrographs of top beads (mid-columnar). A — C_o (6 Al, 5 Ti); B — X (1 Al, 460 Ti); C — Y (660 Al, 4 Ti); D — Z (500 Al, 450 Ti). 2000X.

%. It follows that a better appreciation of microalloying is afforded by quoting concentration in ppm[1] rather than weight percent.

In comparison to earlier studies (Refs. 2, 3), the Ti range was extended from 250 ppm up to almost 500 ppm and, contrary to expectation, no marked degradation in notch toughness was encountered at the higher levels. A sharp reversal was previously (Ref. 2) exhibited in the region of 200 ppm Ti on lowering oxygen and adding 25 ppm B. For Ti-B submerged arc deposits, Okaguchi, *et al.* (Ref. 19), established that the correct quantity of Ti, for peak toughness, is linked to oxygen content at a Ti/O ratio of 0.9. Pokhodnya, *et al.* (Ref. 5), on the other hand, investigating UONI-13/55 electrodes yielding 110 to 420 ppm Ti, found better toughness at the lower end of the range. Oxygen was practically invariable, but since side plate structures were progressively formed, it is presumed that impairment was due to the fact that the response at 1% Mn differs to that at 1.4% Mn (Ref. 3). Rissone, *et al.* (Ref. 6), also encountered better toughness at 200 ppm than at 500 ppm Ti, but a nitrogen drift occurred as a consequence of using nitrogen containing Fe-Ti as the titanium source. With no Fe-Ti addition, the microstructure was nonacicular and it is feasible, within analytical scatter, that the Ti content was actually less than the quoted value of 20 ppm. In retrospect, it is evident that increments of the order of 10 ppm are required to locate the highly effective concentration peak occuring at 30 - 40 ppm Ti. Furthermore, it is now apparent that the Mn-Ti model presented previously Ref (3) was truncated and that, in the absence of other micro-alloying elements, up to 400 ppm Ti can be tolerated for the specific welding conditions employed.

The individual addition of Al and Ti powder necessitated that the amount of Fe-Si in the coating be progressively decreased, so as to maintain the weld metal silicon content constant. Similarly, in the mixed system, the addition of Al required that the titanium powder be also decreased, so as to maintain a stable concentration of titanium in the weld. The overall deoxidation potential was thus affected with the result that the weld oxygen level was not stabilized. At 40 ppm Ti a balance existed such that oxygen remained constant with increasing Al content. The inclusion composition (Ref. 4), on the other hand, changed progressively from manganese silicate to alumina, but with little change in average inclusion size. On further addition of titanium, the inclusions became compounds of titanium and aluminum, of mixed composition, and trapped, in some cases, as large

1. One part per million (ppm) = 0.0001%.

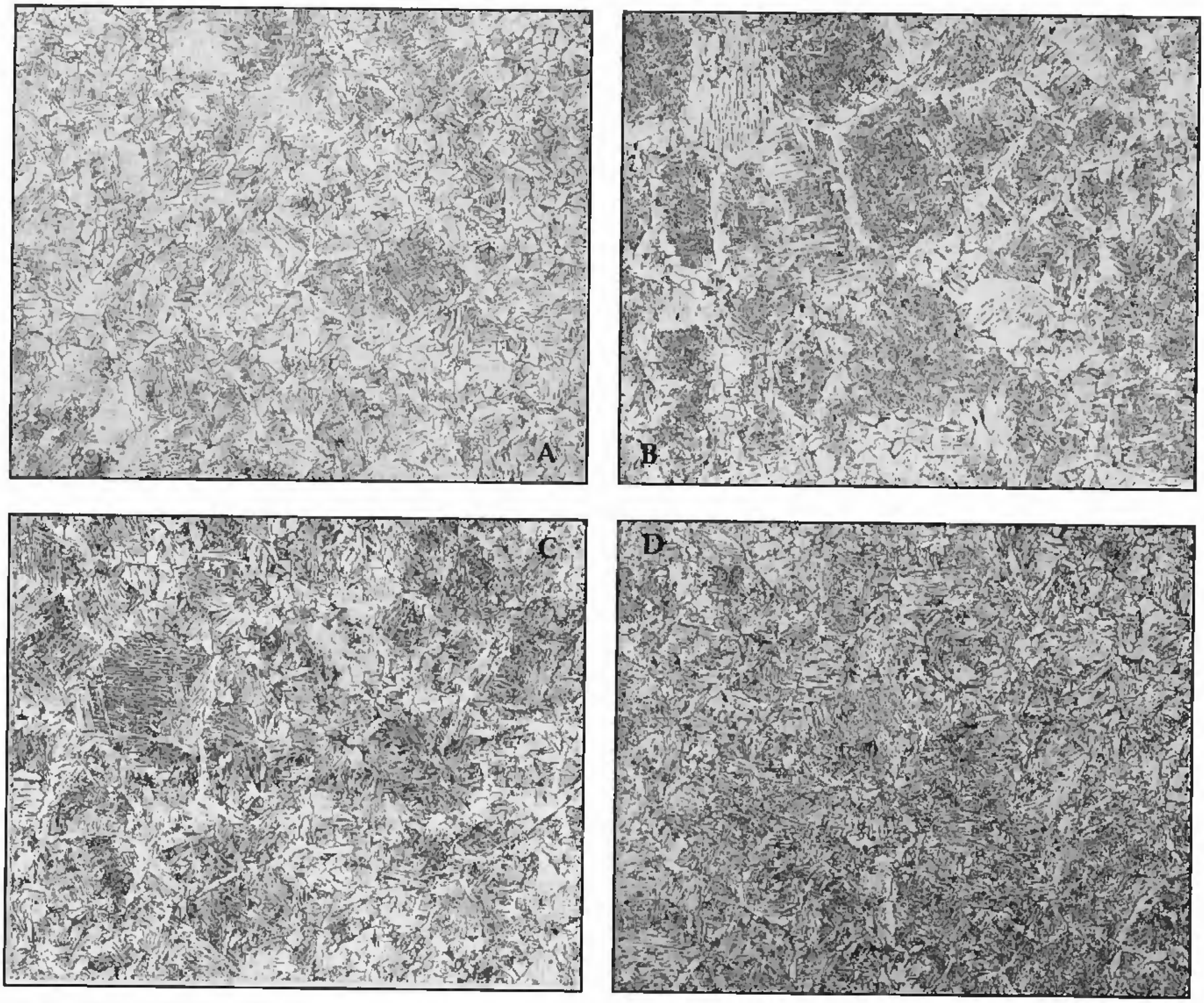

Fig. 6 — Photomicrographs of high-temperature reheated regions. A — C_o (6 Al, 5 Ti); B — X (1 Al, 460 Ti); C — Y (660 Al, 4 Ti); D — Z (500 Al, 450 Ti). 200X.

cubic particles. In basic submerged arc weld metal, Al-induced coarsening of inclusions has been accounted (Ref. 10) for as being due to nucleation at a higher temperature leading to longer times to coalesce before solidification. Of note also, for the same process, is that Kayali, *et al.* (Ref. 31), found that very high Ti welds, with intermediate levels of Al, contained inclusions of more distinct shapes than low-Ti welds.

The microstructural studies of the as-deposited weld metal revealed that Al and Ti, when added individually, have markedly different effects on intragranular acicular ferrite nucleation, the increase in the volume fraction of AF being twofold and sevenfold, respectively, at the 500 ppm concentration level. In accord with Devillers, *et al.* (Ref. 12), it is confirmed, by inference from previous inclusion analysis (Ref. 4), that alumina particles are not efficient promoters of acicularity. Titanium compounds, on the other hand, located at the surface of silicate inclusions are widely accepted (Refs. 22, 27, 30, 32) as being highly effective nucleants. A cyclic phenomenon was previously encountered (Ref. 3), dependent on Mn content, with an initial dramatic increase in acicular ferrite being reversed at titanium levels in excess of 40 ppm. The reason for the reversal remains enigmatic, but it is tentatively assumed that the TiO phase (Ref. 33) at the interface is either thickened or modified over the intermediate range up to 80 ppm Ti. On increasing the TiO content of the inclusions to more than 10% (Ref. 2), AF increased again, and in all probability, other compounds in the form of spinels became operative. Thus, it appears that in the present mixed system adding up to 60 ppm Al, at low and intermediate levels of Ti, served in a similar manner to obviate to a certain extent the beneficial effect of titanium. Then between 60 and 160 ppm Al, the situation improved, with AF increasing due to the formation of mixed compounds of the two elements. Subsequently, at 160 ppm Al, a further reversal occurred, with excess Al possibly going into solution, as described by Terashima and Hart (Ref. 14), for submerged arc weldments. At the highest titanium level, *i.e.*, 450 ppm, a

Table 2 — Semiquantitative Analysis of Inclusions (%)

Al	Si	Ti	Mn	Fe
21.71	12.96	65.32	—	—
62.79	—	26.42	5.61	5.16
70.37	1.55	14.16	9.03	4.87
27.34	1.73	64.18	4.91	1.82
80.55	—	10.59	7.88	0.98
60.78	0.92	30.19	6.95	1.13
70.87	1.35	25.22	1.04	1.50

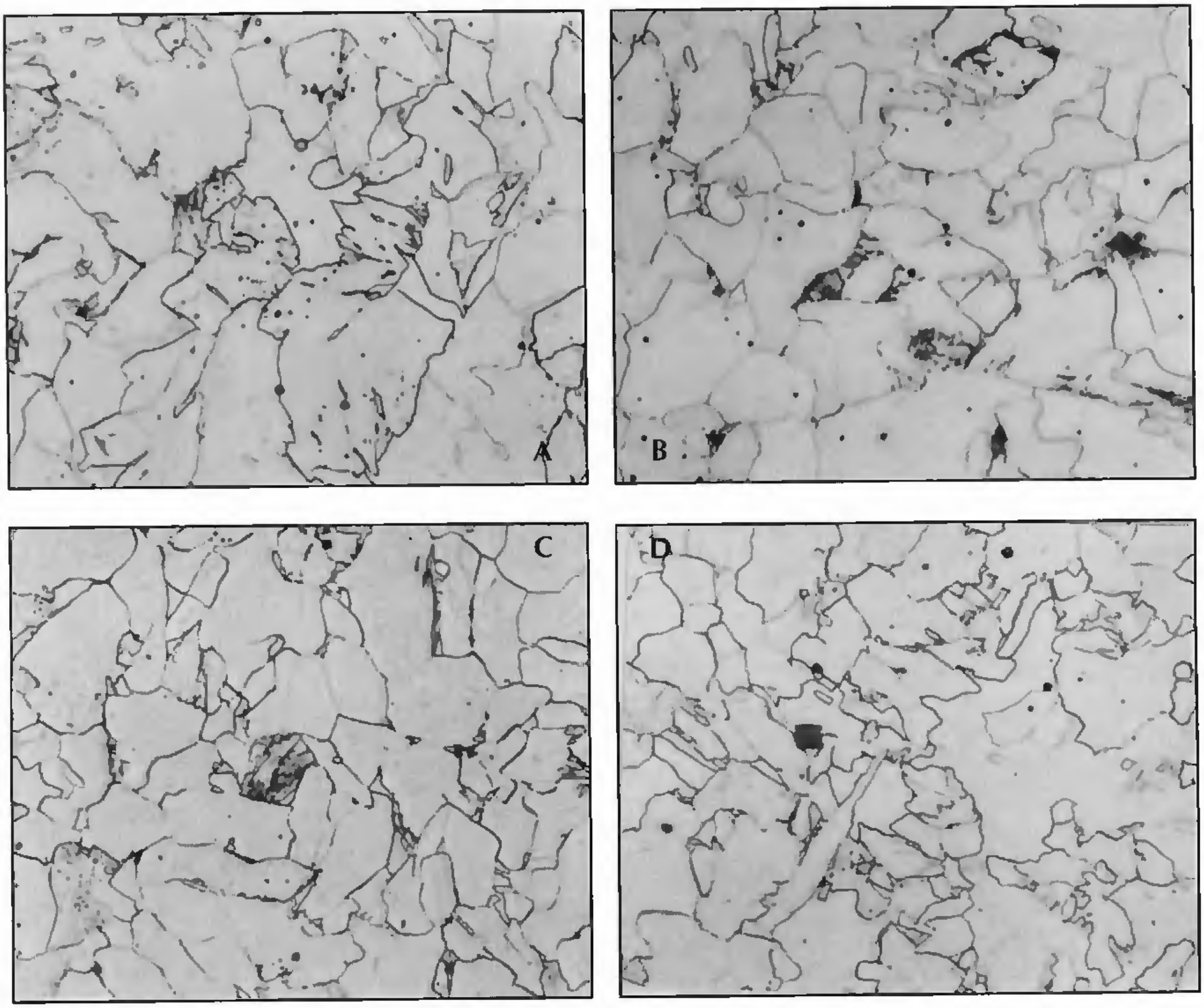

Fig. 7 — Photomicrographs of low-temperature reheated regions. A — C_o (6 Al, 5 Ti); B — X (1 Al, 460 Ti); C — Y (660 Al, 4 Ti); D — Z (500 Al, 450 Ti). 200X.

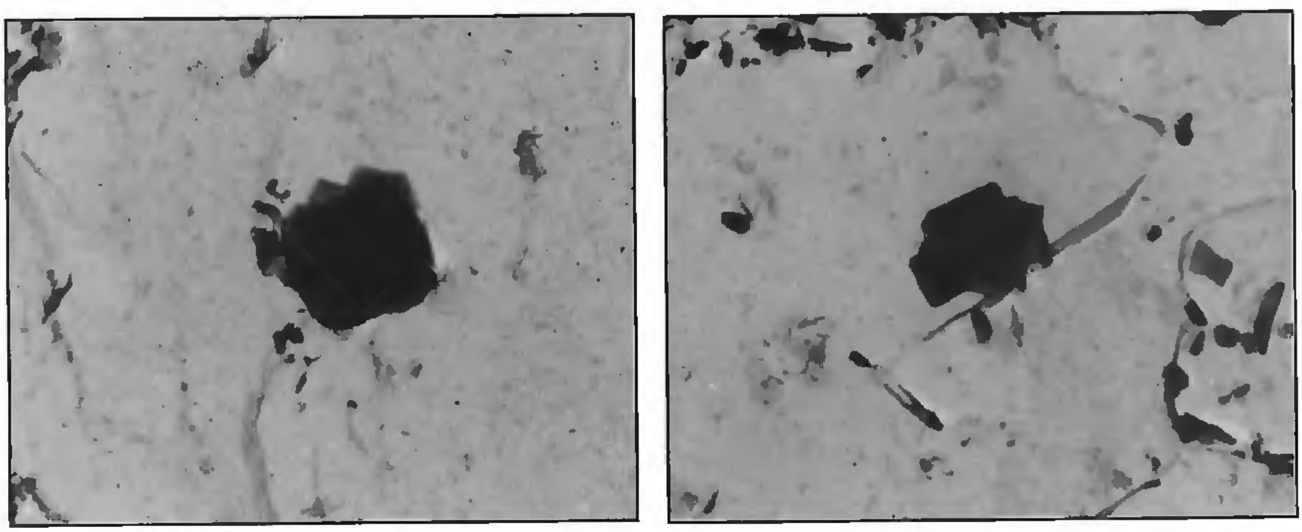

Fig. 8 — Single and multiple cubic particles. Z. 20,000X.

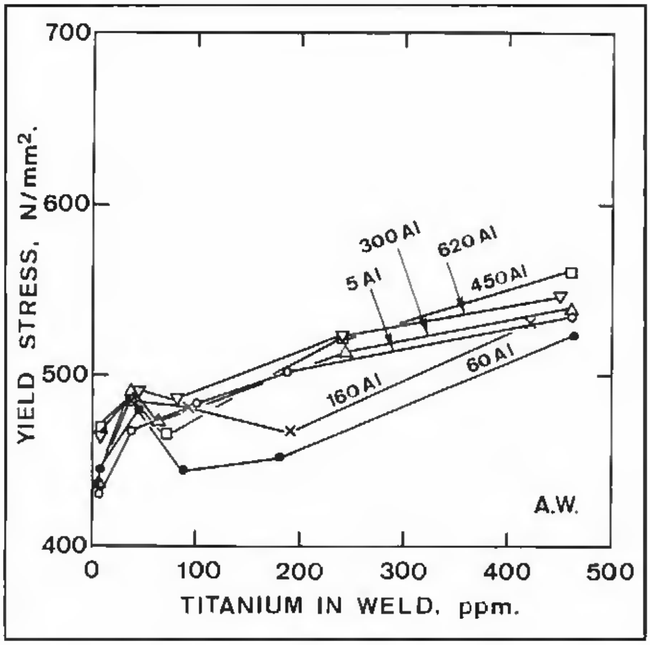

Fig. 9 — Effect of titanium on yield strength (different aluminum levels).

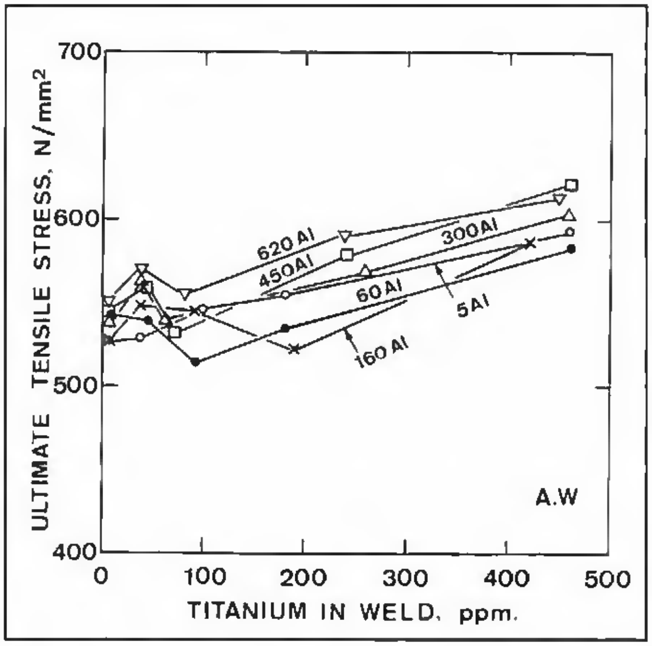

Fig. 10 — Effect of titanium on ultimate tensile strength (different aluminum levels).

different situation existed, with aluminium addition tending to slightly increase the amount of AF. Thus, the compositional change to the inclusions and the formation of large cubic particles seem to have had little effect on the transformation characteristics.

Microalloying influenced the microstructure of the high-temperature reheated regions, with equivalent changes in acicularity tending, in the main, to occur in the top beads. The structure of the low-temperature reheated regions also underwent modification with a change in grain size and microphase morphology being observed. The overall effect on bulk tensile properties, especially yield strength, was complex with an initial sharp peak, at 40 ppm Ti, being followed by a generally increasing trend. For Al, a different situation was encountered with an initial decrease down to 60 ppm Al being followed by a subsequent increase. In contrast to the case for C and Mn in combination (Ref. 34), for example, no attempt was made to apply a regression analysis to the data. At this stage, it would appear difficult to develop a general predictive model for tensile parameters, bearing in mind the additional interactive influence of Mn on the titanium effect (Ref. 3).

Notch impact toughness within the system varied substantially, the Charpy V-notch test temperature for 100 J ranging from −15° to −72°C (5° to −97.6°F). Aluminum addition, at the 60 ppm level, induced a degradation in toughness, whereas titanium, at the 40 ppm level, was beneficial. The observed trends, depicted in a three-dimensional form (Fig. 13), indicate a precipitous transverse drop, to lower temperatures, due to Ti and a longitudinal ridge, induced by the addition of Al, culminating in a point of poor toughness at 60 ppm Al and 100 ppm Ti. Additionally, at 350 ppm Al and 35 ppm Ti, a dip is indicated, with good toughness properties being achieved prior to impairment by further addition of both elements. The vertical side wall and the ridge, in the depicted model, reflect obversely, to a certain extent, the changes in the volume fraction of AF in the top beads. No direct correlation exists, however, for the complete system, since the cyclic toughness changes are indicative of bulk properties, with a high degree of recrystallization (75–80%) (Refs. 1–4). Thus, for the extreme composition (Z), where the AF content of the as-deposited metal was high, the toughness was relatively poor due to the morphology of the microphases in the reheated regions. The oxygen imbalance would naturally skew the depicted surface of the model, and it is presumed that the large cubic particles present would be damaging for toughness.

The role of weld oxygen content was separately investigated by additionally mixing different amounts of Mg powder with the Al in the coating. The weld titanium content was maintained constant, at the previous level of 35 ppm (Ref. 4), and oxygen was progressively reduced from 430 down to 320 ppm. The comparative notch toughness results are plotted in Fig. 14 and show that the reversal encountered at 350 ppm Al was displaced to 160 ppm Al, on lowering oxygen. A compression of the three domains referred to previously (Ref. 4) occurred, with 100 J at −84°C being attained at the optimum. Rather incongruously, the Al : O ratio at the reversal also changed, from 0.8 to 0.5. As noted initially (Ref. 4), maximum toughness did not coincide with the AF peak, which was found at 160 ppm Al. In accord with Thewlis (Ref. 35), it would appear that the galaxite spinel ($Al_2O_3 \cdot MnO$) is particularly effective in influencing transformation kinetics. A trace of titanium is still a requisite, however, as found by Saggese, *et al.* (Ref. 36), and demonstrated in Fig. 11, for 160 ppm Al. Subsequent to the addition of 36 ppm Ti, little sensitivity to a further increase in Ti is indicated for this aluminum level. For submerged arc welding, Terashima and Hart (Ref. 14) found that basic fluxes, in contrast to a calcium silicate flux, responded critically to excess Al diluted from the base plate, an increase from 200 to 300 ppm Al inducing a lateral shift in transition temperature of +100°C. In view of the required balance with oxygen, it appears more opportune, for low heat input plain C-Mn SMA deposits, to rely on the aluminum-free system, containing the correct amount of Ti.

Apart from oxygen, weld metal nitrogen content is also naturally important in defining the surface profile of the toughness model — Fig. 13. This aspect was additionally investigated by introducing different amounts of nitrided manganese metal into the coatings, so as to attain two further levels of nitrogen. Comparative toughness data, for an aluminum and

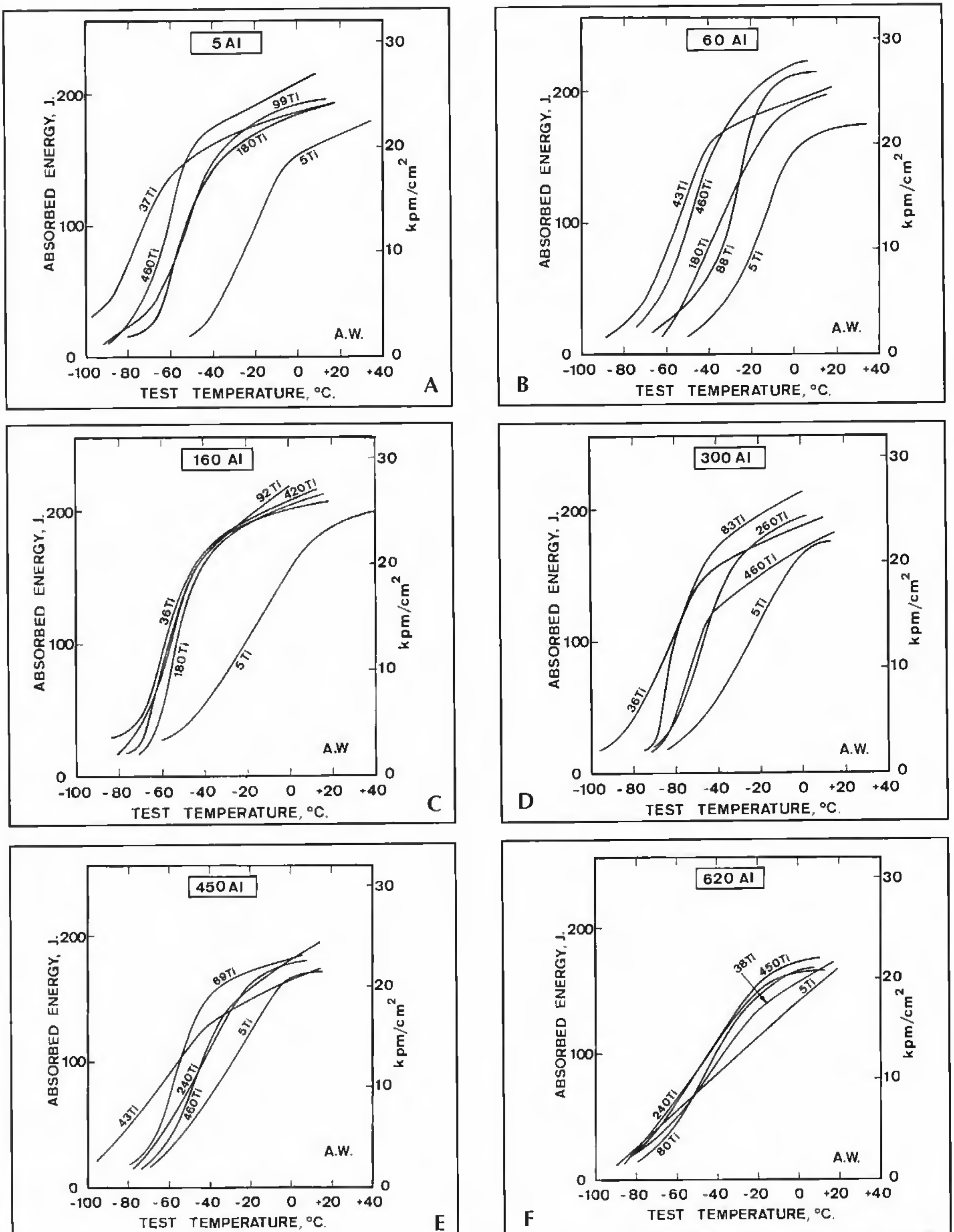

Fig. 11 — Charpy V-notch impact curves for deposits containing different titanium contents. A — 5 Al; B — 60 Al; C — 160 Al; D — 300 Al; E — 450 Al; F — 620 Al.

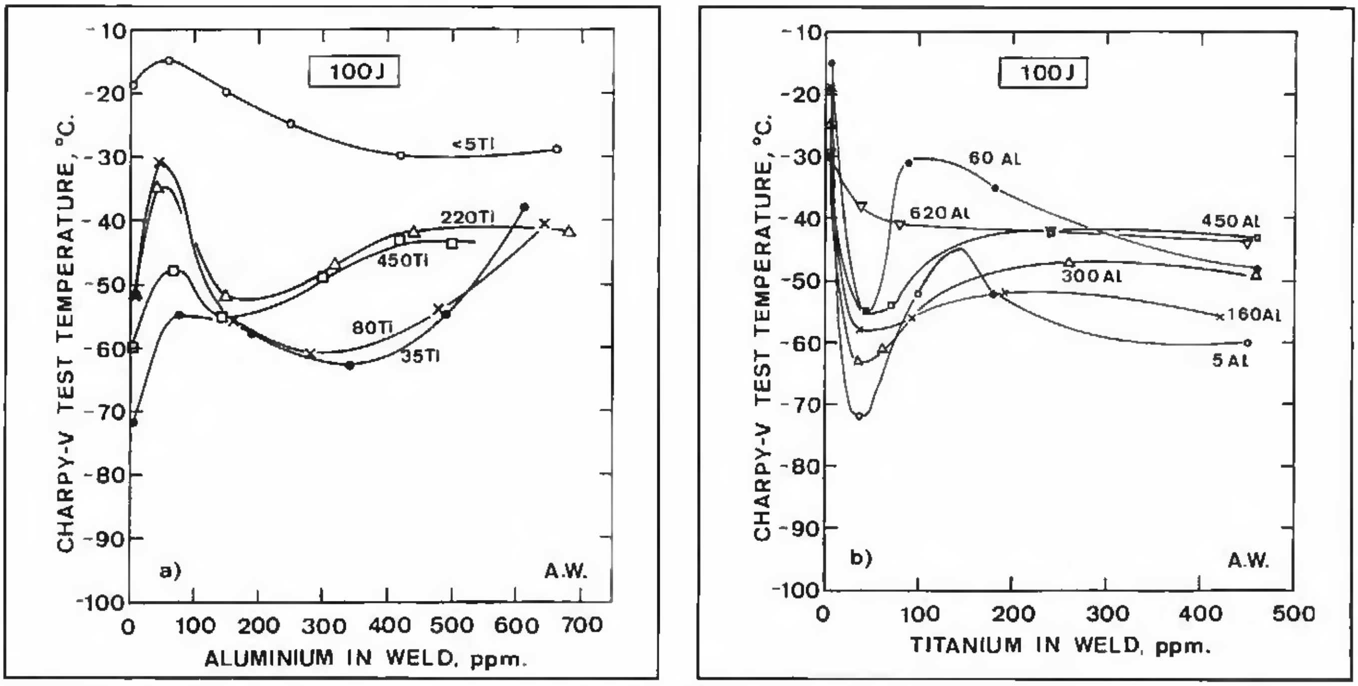

Fig. 12 — Charpy V-notch test temperature corresponding to 100 J plotted vs. Al and Ti content. A — Al content; B — Ti content.

a titanium series, are shown in Fig. 15A and B, respectively. A considerable displacement to higher temperatures is seen to have occurred, with a tendency for the peaks to be dampened. Of note is the fact that the optimum titanium content was displaced toward 50 ppm as the nitrogen increased.

An investigation is currently underway to evaluate the effect of titanium in combination with up to 200 ppm B. Also, Al is being further added in order to study the response of the TiBAl system to nitrogen, in both the as-welded and the strain-aged condition. Microanalysis of the nonmetallic inclusions is being conducted, with particular regard to the concentration of the light elements (Ref. 33). Furthermore, CTOD and wide plate tests are being carried out on welds of specifically chosen compositions.

Conclusions

For weld deposits containing 1.4% Mn, the following applied:

Titanium addition, in contrast to aluminum, dramatically enhanced the formation of acicular ferrite and improved notch toughness.

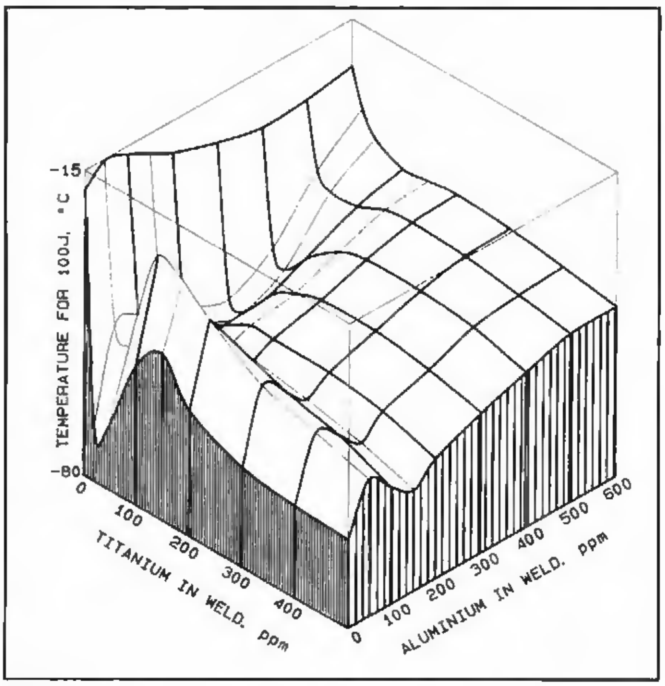

Fig. 13 — Notch toughness model of the Al-Ti system (AW).

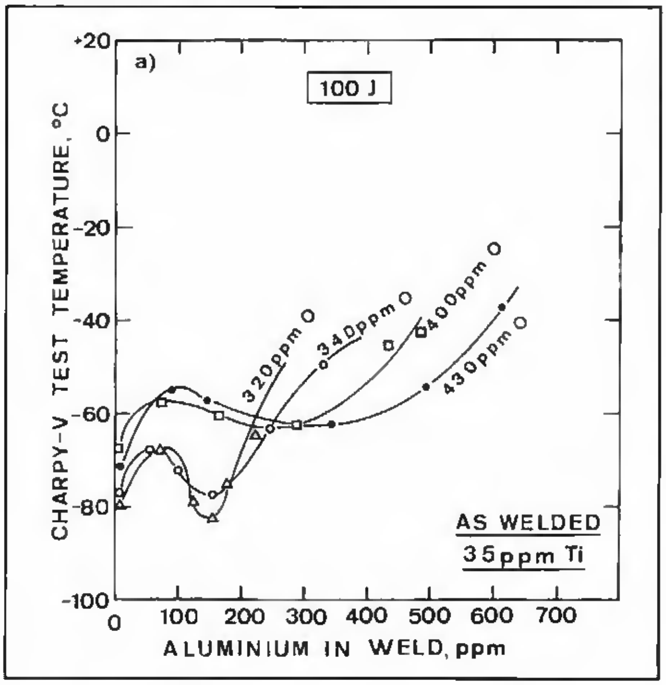

Fig. 14 — Effect of aluminum at different weld oxygen levels.

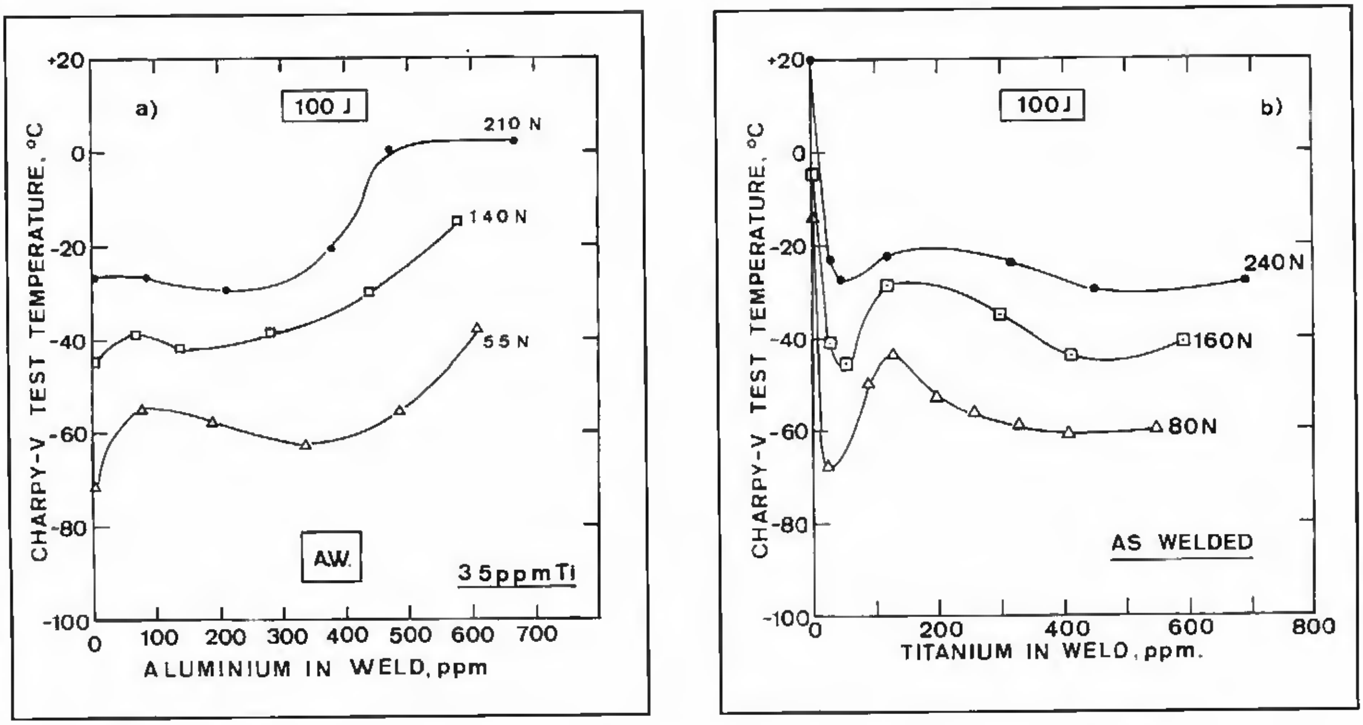

Fig. 15 — Effect of aluminum and titanium at different weld nitrogen levels. A — aluminum; B — titanium.

Table 3 — Mechanical Test Results

Nominal Ti ppm	Al ppm	YS N/mm²	UTS N/mm²	El %	RA %	ISO-V Temp. °C 100 J	ISO-V Temp. °C 28 J
5	6	431	527	29.6	78.0	−19	−41
	60	444	542	27.6	72.9	−15	−39
	150	437	527	24.6	78.9	−20	−58
	250	437	538	25.2	78.9	−25	−56
	420	469	545	24.4	77.0	−30	−62
	660	466	551	26.2	78.9	−29	−76
40	5	468	529	32.6	80.7	−72	−99
	78	478	540	31.2	80.7	−55	−77
	190	485	549	31.4	79.8	−58	−86
	340	491	564	28.2	78.9	−63	−88
	490	485	560	25.2	78.9	−55	−90
	610	491	570	29.2	77.0	−38	−74
80	8	484	547	29.4	79.8	−52	−74
	47	442	514	32.2	81.6	−31	−57
	160	481	545	30.6	81.4	−56	−68
	280	474	540	28.0	80.7	−61	−68
	480	466	533	27.2	77.0	−54	−70
	640	486	555	26.6	78.0	−41	−68
220	3	502	555	26.6	78.9	−52	−67
	47	452	535	30.7	78.9	−35	−54
	150	467	522	29.2	77.0	−52	−64
	320	514	570	23.6	77.0	−47	−63
	440	522	580	24.0	76.0	−42	−68
	680	522	591	23.8	71.9	−42	−76
450	1	535	594	26.0	79.8	−60	−78
	67	522	583	22.0	78.9	−48	−69
	150	531	587	25.2	78.0	−56	−74
	300	538	604	23.2	77.0	−49	−65
	420	561	622	26.0	77.0	−43	−63
	500	547	616	22.6	75.0	−44	−76

Aluminum addition, up to a level of 60 ppm tended to limit the beneficial influence of titanium.

Intermediate levels of aluminum, in combination with a small amount of titanium, induced an improvement.

Unless a balance is achieved, with regard to oxygen, then aluminum should be maintained as low as possible and titanium optimized at 30 to 40 ppm.

Acknowledgments

Thanks are extended to R. Zullig for assistance with the metallography. The nonmetallic inclusions were analyzed, under contract, by J. Bosansky, Welding Research Institute, Bratislava, Slovakia.

References

1. Evans, G. M. 1993. The effect of microalloying elements in C-Mn steels weld metal. *Welding in the World* 31(1): 12–19.

2. Evans, G. M. 1992. The effect of titanium in SMA C-Mn steel multipass deposits. *Welding Journal* 71(12): 447-s to 454-s.

3. Evans, G. M. 1993. The effect of titanium in manganese-containing SMA weld deposits. *Welding Journal* 72(3): 123-s to 133-s.

4. Evans, G. M. 1991. The effect of aluminum in shielded metal arc C-Mn steel multipass deposits. *Welding Journal* 70 (1): 32-s to 39-s.

5. Pokhodnya, I. X., Korsun, A. O., and Meshkov, Yu Ya. 1987. Effects of titanium added to the coating of UONI-13/55 electrodes on the microstructure and mechanical properties of the weld metal. *Welding International* 1 (9): 806 – 811.

6. Rissone, N. M., Rissone, H. A., Zuliani, J. L., and Timerman, R. Effect of titanium on the properties of manual multipass welds. IIW Doc. II-A-665-85.

7. North, T. H., Bell, H. B., Nowicki, A., and Craig I. 1978. Slag-metal interaction, oxygen content and toughness during submerged arc welding. *Welding Journal* 57 (4): 63-s to 75-s.

8. North, T. H., Bell, H. B. Koukabi, A., and Craig, I. 1979. Notch toughness of low-oxygen content submerged arc deposits. *Welding Journal* 58(12): 343-s to 354-s.

9. Thaulow, C. 1980. Structural changes in submerged arc weld metals of C-Mn steels containing small amounts of titanium. *Proc. Int. Conf., Weld Pool Chemistry and Metallurgy*. TWI, London, Paper 29.

10. Hannerz, N. E., and Werlefors, T. 1980. The influence of parent material aluminium content on microstructure, inclusion distribution, and mechanical properties of submerged arc weld metal. *ibid*, Paper 43.

11. Snyder, J. P., and Pense, A. W. 1982. The effect of titanium on submerged arc weld metal. *Welding Journal* 61 (7): 201-s to 211-s.

12. Devillers, L., Kaplan, D., Marandet, B., Ribes, A., and Ribound, P. V. 1983. The effect of low level concentrations of some elements on the toughness of submerged arc welded C-Mn steel welds. *Proc. Int. Conf., Effects of Residual, Impurity and Microalloying Elements*, TWI, London, Paper 1.

13. Bonnet, C., and Charpentier, J-P. 1983. Effect of deoxidation residues in wire and of some particular oxides in CS fused fluxes on the microstructure of submerged arc weld metals. *ibid*, Paper 8.

14. Terashima, H., and Hart, P. H. M. 1984. Effect of aluminum on C-Mn-Nb steel submerged arc weld metal properties. *Welding Journal* 63(6): 173-s to 183-s.

15. Oldland, R. B. 1985. The influence of aluminium and nitrogen on the microstructures and properties of single pass submerged arc welds. *Australian Weld. Res.*, 14: 44–56.

16. Heintze, G. N., and McPherson, R. 1986. Solidification control of submerged arc welds in steels by inoculation with Ti. *Welding Journal* 65(3): 71-s to 82-s.

17. Brownlee, J. K., Matlock, D. K., and Edwards, G. R. 1986. Effects of aluminum and titanium on the microstructure and properties of microalloyed steel weld metal. *Proc. Int. Conf Advances in Welding Science and Technology*, ASM, Gatlinburg, Tenn., pp. 245–250.

18. Burkhardt, J., Lau, T., North, T. H., and L'Esperance, G. 1988. Effect of aluminum on the Ti-O-B-N balance in submerged arc welding. *Welding Journal* 67(8): 25–30.

19. Okaguchi S., Kushida, T., Fukada, Y., and Tanaka, S. 1990. Recent development of sour-gas service line pipe for North Sea use. *The Sumitomo Search* (43): 25–34.

20. Boniszewski, T. 1969. Titanium in steel wires for CO_2 welding. *Met. Constr.* 1(5): 225–229.

21. Ul'Yanov, V. I., Parfessa, G. I. and Shevchuk, R. N. Effects of the aluminium in electrode wire on the strength of CO_2 weld metal. *Autom. Weld.* 24(12): 14–18.

22. Ohkita, S., Homma, Tsushima, S., and Mori, N. 1984. The effect of oxide inclusion on microstructure of Ti-B containing weld metal. *Australian Welding Journal* 28: 29–36.

23. Widgery, D. J. 1974. Deoxidation practice and toughness of mild steel weld metal. *Weld. Res. Int.* 4: 54–80.

24. Hart, P. H. M., and Hutt, G. A. 1986. An investigation into the factors influencing mechanized MIG weld metal toughness. *Proc. Int. Conf., Welding and Performance of Pipelines*, London, TWI, Paper 71.

25. Kluken, A. O., and Grong, O. Mechanism of inclusion formation in Al-Ti-Si-Mn deoxidized steel weld metals. *Met. Trans. A.* 20A, pp. 1335–1349.

26. Abson, D. J. 1992. The influence of aluminium additions to tubular cored welding electrodes on the microstructure and toughness of as-deposited C-Mn-Ni weld metal. *TWI Journal* 1(1): 100–115.

27. Abson, D. J. 1989. Nonmetallic inclusions in ferritic steel weld metals — a review. *Welding in the World* 27 (3/4): 76–101.

28. Evans, G. M. 1983. Factors affecting the microstructure and properties of C-Mn all-weld-metal deposits. *Weld. Res. Abroad*, WRC, 29(1): 2–69.

29. Guidelines for classification of ferritic steel weld metal microstructural constituents using the light microscope. *Weld. in the World* 24(7/8): 144–149.

30. Grong, O., and Matlock, D. K. 1986. Microstructural development in mild and low alloy steel weld metals. *Int. Metals Reviews* 31(1): 27–48.

31. Kayali, E. S., Corbett, J. M., and Kerr, H. W. 1983. Observations on inclusions and acicular ferrite nucleation in submerged arc HSLA welds. *J. Mat. Science Letters* 2(3): 123–128.

32. Es-Souni, M., and Beaven, P. A. 1990. Microanalysis of inclusion/matrix interfaces in weld metals. *Surface and Interface Analysis* 16: 504–509.

33. St-Laurent, S., and L'Esperance, G. 1992. Effect of N, B and Ti on the microstructure and toughness of C-Mn weld deposits. *Proc. Int. Conference, Advances in Welding Science and Technology*, ASM, Gatlinburg, Tenn., pp. 527–531.

34. Evans, G. M. 1983. The effect of carbon on the microstructure and properties of C-Mn all-weld metal deposits. *Welding Journal* 62(11): 313-s to 320-s.

35. Thewlis, G. Transformation kinetics of ferrous weld metals. *Materials Science and Technology*, to be published.

36. Saggese, M. E., Bhatti, A. R., Hawkins, D. N., and Whiteman, J. A. 1983. Factors influencing inclusion chemistry and microstructure in submerged arc welds. *Proc. Int. Conf. Effect of Residual, Impurity and Microalloying Elements*. The Welding Institute, London, Paper 15.

37. Evans, G. M. 1982. The effect of heat input on the microstructure and properties of C-Mn all-weld-metal deposits, *Welding Journal* 61(4): 125-s to 132-s.